Energy Conversion and Management 97 (2015) 409–419

Contents lists available at ScienceDirect

Energy Conversion and Management

journal homepage: www.elsevier.com/locate/enconman

Exploring switchgrass and hardwood combustion on excess air and ash fouling/slagging potential: Laboratory combustion test and thermogravimetric kinetic analysis

Yu Wang [a,b,c], Yixin Shao [b], Miodrag Darko Matovic [c], Joann K. Whalen [a,*]

[a] Department of Natural Resource Sciences, McGill University, Ste-Anne-de-Bellevue, Quebec, Canada
[b] Department of Civil Engineering and Applied Mechanics, McGill University, Montreal, Quebec, Canada
[c] Department of Mechanical and Materials Engineering, Queen's University, Kingston, Ontario, Canada

ARTICLE INFO

Article history:
Received 8 December 2014
Accepted 19 March 2015

Keywords:
Biomass fuel
Combustion
Thermogravimetric kinetics
Ash fouling/slagging
Excess air ratio

ABSTRACT

Biomass combustion generates renewable energy, which is optimized by designing a biomass combustion system that controls excess air intake and evaluates the ash fouling/slagging potential. The objective of this study was to (1) investigate the effect of excess air ratio (EAR) on the combustion of switchgrass (*Panicum vigratum L.*) and hardwood, (2) assess their ash fouling and slagging tendencies, and (3) perform an in-depth thermogravimetric kinetic analysis to understand their combustion. Switchgrass and hardwood contained 17.5 and 17.7 MJ/kg of energy value, which was appropriate for heat generation. The greatest energy conversion efficiency and combustion completeness rate were obtained with an EAR of 20% for switchgrass and 30% for hardwood based on our combustion system with 4 mm particles of fuel. Kinetic analysis confirmed that increasing the oxygen availability resulted in superior energy conversion. In general, switchgrass ash had lower fouling and slagging tendencies than hardwood owing to its more acidic chemical composition. Heat and mass transfer delays were still observed from this combustion system, thus making the combustion request more air to even achieve a stoichiometric condition. However, rather than an ideal test (e.g. single particle combustion), the conclusions made by this study were a practical guidance for boiler operations, since the heat and mass transfer delays were a common phenomenon in real applications that should not be eliminated in our lab-scale studies.

1. Introduction

Switching to biomass fuel has the potential to lower the carbon footprint in many industries because biomass is carbon–neutral, compared to fossil fuels such as coal [1,2]. Energy conversion from biomass fuel is readily achieved by direct combustion, an exothermic chemical reaction between carbohydrate material and oxygen [3]. Compared to other common biomass energy conversions (e.g. gasification or pyrolysis), direct combustion requires little extra infrastructure when fossil fuel is switched to biomass fuel [4]. Thus, it is more technically feasible and has lower capital cost particularly for large power levels [5]. The air intake at combustion determines the energy conversion and emissions from biomass [6]. Insufficient air causes more CO emission and inferior energy efficiency due to unburnt carbon [7]. However, there are many factors in boilers that decrease the air utilization efficiency and retard the combustion completeness, such as the heat and mass transfer delays. Hence, a biomass boiler typically incorporates 10–30% of excess air (EAR = 1.1–1.3) (Eq. (1)), above that required by stoichiometric condition (EAR = 1.0), to maximize the energy output [8]. Yet, a high input of excess air in boilers will actually lower the combustion temperature, thereby degrading the theoretical energy efficiency according to the Carnot thermodynamic cycle.

$$\text{Excess air ratio (EAR)} = \frac{\text{Actual air supply}}{\text{Air demand at stoichiometric condition}} \quad (1)$$

Another crucial factor in biomass combustion is ash deposition. Alkali metals (Na_2O and K_2O) in biomass can react with SiO_2 to form alkali silicate that melts at below 700 °C. When these sticky particles adhere to the cooler surface of the combustor, it results in a fouling problem [9]. Meanwhile, Na_2O and K_2O also react with sulfur if the temperature is above 700 °C, which forms alkali sulfate

* Corresponding author at: Department of Natural Resource Sciences, Macdonald Campus of McGill University, 21111 Lakeshore Road, Ste-Anne-de-Bellevue, Quebec H9X 3V9, Canada. Tel.: +1 514 398 7943; fax: +1 514 398 7990.
E-mail address: joann.whalen@mcgill.ca (J.K. Whalen).

http://dx.doi.org/10.1016/j.enconman.2015.03.070
0196-8904/

Nomenclature

EAR	excess air ratio, 1	m_f	final solid mass, mg
SAFR	stoichiometric air-fuel ratio, 1	$f(\alpha)$	solid-state reaction mechanism function
$V(t)$	gaseous volume concentration, %	A	Arrhenius pre-exponential factor, min^{-1}
N	gaseous molecular mass, g/mol	k	solid-state reaction rate, t^{-1}
S	volume velocity of exhaust, L/s	t	solid-state reaction time, min
M_f	fuel load mass, g	E_a	Arrhenius activation energy, kJ/mol
ECE	energy conversion efficiency, %	T	absolute temperature, K
CCR	combustion completeness rate, %/min	R	gas constant, J/mol K
α	decomposition rate, 1	$g(\alpha)$	integral function of solid-state reaction mechanism $f(\alpha)$
m_0	initial solid mass, mg	β	heating rate, K/min
m_t	solid mass at time t, mg		

that deposits on the heat transfer surface (slagging problem) [10]. Fouling and slagging reduce the heat transfer and accelerate corrosion of the combustor walls [11,12]. Thus, some empirical indices were developed to assess the fouling and slagging tendencies of biomass fuel, including basic-acid ratio (BA), fouling index (FI), slagging index (SI) and slag viscosity ratio (SVR) [13]. These predictive indices have proved consistent with real observation of combustion systems those were fed with woody and agricultural waste [14], straw and wood pellet [13] and sewage sludge [15]. Hence, the fouling and slagging tendencies of biomass fuels need to be considered in designing biomass combustion systems.

Several biomass fuels are emerging as substitutes for fossil fuels in eastern Canada due to the suitable climate and acreage available for their growth, including switchgrass and hardwood residues [16]. Switchgrass is a perennial warm-season bunchgrass that yields up to 25 tonnes of dry matter per hectare [17]. It is rich in volatile content (70.1–85.2%) and has an excellent calorific value (18.0–26.2 MJ/kg) [18]. Hardwood residues are forestry wastes from sawmills and other forestry operations that have a great gross energy value compared to conventional biomass [19], such as poplar (18.5 MJ/kg), cereal straw (17.3 MJ/kg) or bagasse (19.4 MJ/kg) [20]. Although combustion of these fuels was studied, including fuel characterization [21], emissions [22], ash properties [23] and combustion optimization [24], we are not aware of any published work that examined how excess air affects their combustion, and the fouling and slagging risks of these fuels in biomass combustion systems.

Empirical data can be obtained from pilot-scale combustion systems where switchgrass or hardwood residues are the fuel sources, but such data is specific to the operating system and cannot be extrapolated to larger-scale biomass combustors. Kinetic analysis generates information that can be scaled up to optimize the function of commercial-scale biomass combustion systems in real-time [25]. For instance, choosing the right temperature to optimize the energy conversion process requires kinetic analysis [26], through methods such as non-isothermal thermogravimetric analysis with the Coats–Redfern algorithm [27,28]. With this method, blends of coal and pine sawdust were studied from 25 to 700 °C with 15 °C/min of heating rate. Coats–Redfern algorithm was applied to determine the kinetic parameters, assuming combustion was a two-state solid-state reaction [29]. Furthermore, this method was also successfully used to investigate the combustion of corn straw [30], peanut–tamarind shells [31], sewage sludge [32], and even polyethylene/polypropylene [33].

This paper aimed to build up a laboratory combustion system to provide some recommendations for real boiler operations. Based on this design, we investigated the effect of excess air (0%, 10%, 20% and 30%) on the combustion of switchgrass and hardwood (4 mm particle size). During these energy conversion processes, we examined the factors including fuel mass loss, temperature and gaseous emissions. Additionally, the ashes from all of these tests were characterized to assess their fouling and slagging tendencies. Furthermore, kinetic analysis of data collected from a non-isothermal thermogravimetric analysis–differential scanning calorimetry (TGA–DSC) provided an in-depth understanding of the combustion properties of switchgrass and hardwood.

2. Material and methods

2.1. Materials preparation and characterization

Switchgrass was collected from Williamsburg and hardwood residues (made of sawdust, free of additives) were gathered from Groupe Savoie Inc., Canada. Subsamples of each residue were pulverized with a Pellet Pros Electric 1000E hammer mill to ≈4 mm of particle size (No. 5 mesh) and all analyses were performed in triplicate. About 10 mg of ground sample was tested by the sequential thermogravimetric method for proximate analysis. Ultimate analysis was performed on about 25 mg of ground sample by microcombustion with a Carlo Erba EA 1108 elemental analyzer. Sulfur content was measured with a HELIOS analyzer at 1350 °C. Higher heating value (HHV) was measured with an oxygen bomb calorific meter. Major mineral oxides and trace metal elements were characterized by the Fusion Inductively Coupled Plasma (Fusion-ICP) with a Varian Vista 735 ICP analyzer. Molecular formula $CH_xO_yN_zS_w$ were determined from the ultimate analysis. Stoichiometric air–fuel ratio (SAFR) was calculated by assuming a stoichiometric combustion of switchgrass and hardwood (Eqs. (2) and (3)) [34].

$$CH_xO_yN_zS_w + \left(1 + \frac{x}{4} + z + w - \frac{y}{2}\right)(O_2 + 3.76N_2) = CO_2 + \frac{x}{2}H_2O + 3.76 \times aN_2 + zNO_2 + wSO_2 \quad (2)$$

$$SAFR = \frac{\left(1 + \frac{x}{4} + z + w - \frac{y}{2}\right) \times 28.97}{12 + x + 16 \times y + 14 \times z + 32 \times w} \quad (3)$$

where we assumed an exact stoichiometric condition for switchgrass or hardwood combustion, and the molecular weight of air was 28.97 g/mol.

2.2. Combustion system

A microscopic combustion system was designed for this study (Figs. 1 and 2). The geometry of combustion chamber was $23.0 \times 30.5 \times 17.0\ cm^3$. A fine mesh-wire basket (400 μm, No. 40 mesh) as a fuel holder ($9.2 \times 9.2 \times 9.2\ cm^3$) was installed inside the combustion chamber. The fine mesh ensured even distribution of air around the fuel. Fuel was ignited by an external torch at the vertical midpoint of fuel holder. To measure the fuel mass loss

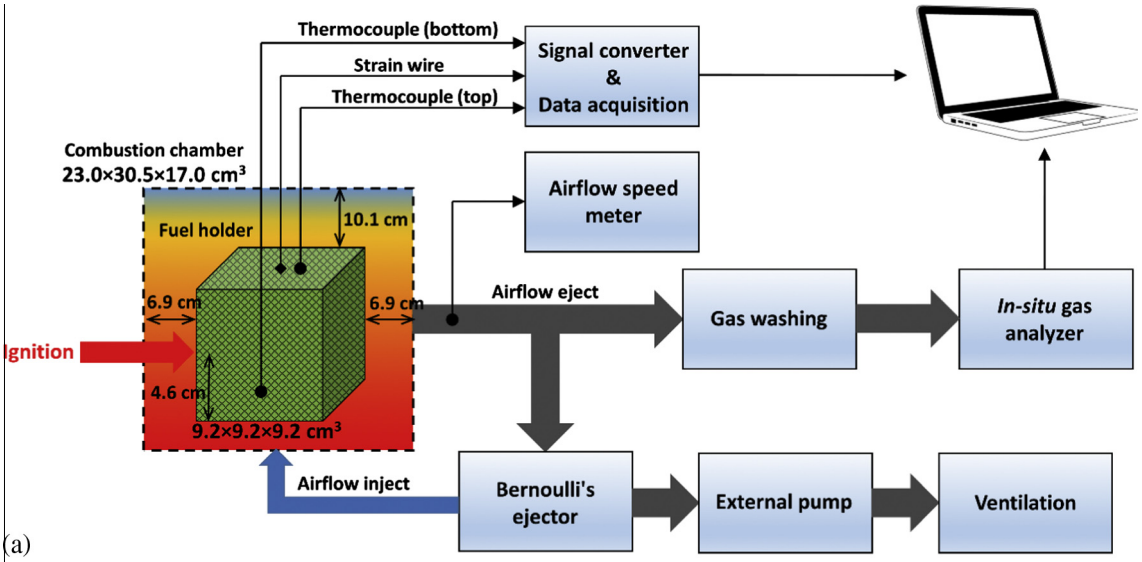

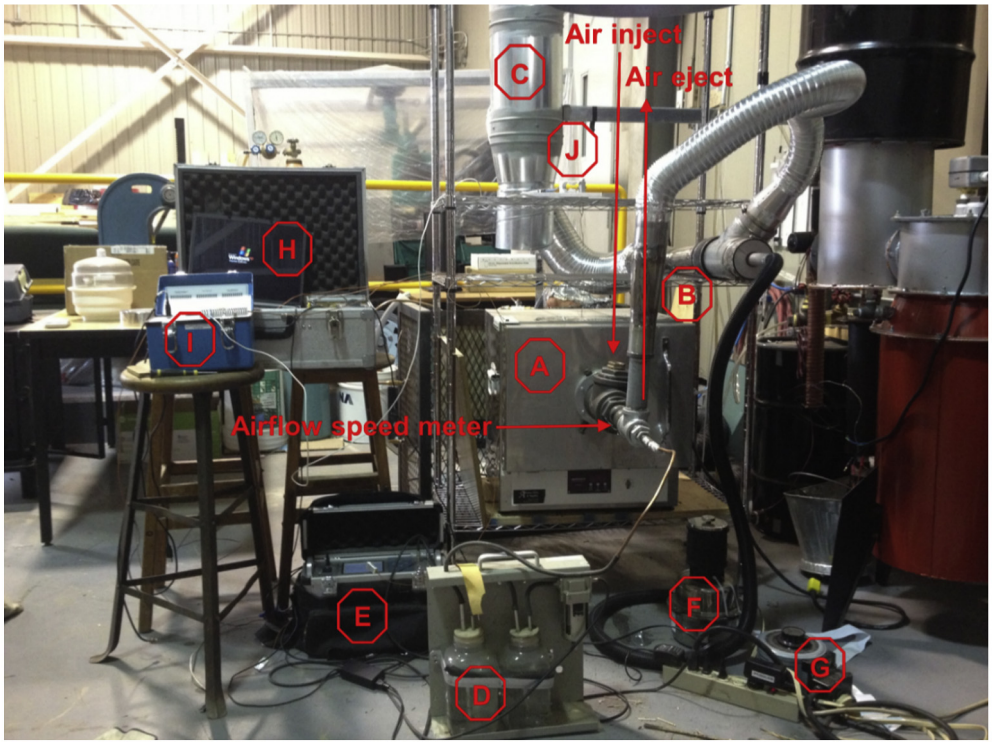

Fig. 1. Schematic diagram (a) and real photo (b) of the biomass fuel experimental combustion system designed for this study. In (b), A: combustion chamber ($23.0 \times 30.5 \times 17.0\ cm^3$ of valid chamber volume); B: Bernoulli's principle air injection and ejection system; C: ventilation system with 9.93 g/min of initial air supply capacity; D: water-washing unit to remove the fine particle and tar from gaseous emissions and to cool down the gas flow for protecting the *in-situ* gas analyzer; E: Gas-board 3100P infrared *in-situ* gas analyzer (CO, CO_2 and O_2); F: an adaptable external pump to provide extra airflow, which could be adjusted by switching different voltage conversion rate; G: an adjustable voltage converter to change the airflow rate from external pump; H: data acquisition system with a signal converter; I: Inter-technology P3 strain indicator and recorder; J: the load cell that was used to measure the mass change of fuel sample.

during combustion, the fuel holder was suspended from an Elane load cell with an Inter-technology P3 strain interpreter. Two thermocouple sensors were placed, one at the bottom and one at the top of the fuel holder. Airflow was expelled through a Bernoulli's ejector with an airflow volume speed sensor [35]. In addition to an initial ventilation unit that provided 9.93 g/min of air, we set up an adaptable pump for extra air supply (Fig. S1). A fine gas sampling pipe was set on the ejector. Emissions (O_2, CO and CO_2) were analyzed by a Gasboard-3100P gas analyzer. All *in situ* measurements were recorded by a data acquisition system.

2.3. Combustion test

Adjusting the pump voltage and initial fuel load permitted control of the EAR from 1.0 to 1.3 (0–30% of excess air) to determine how this parameter affected combustion of switchgrass and hardwood (Table 1). The stoichiometric test with 0% of excess air (1.0 EAR) was considered as the control group. In each test run, biomass was loaded in the fuel holder before combustion. Fuel mass loss and temperature change were monitored throughout a 90 min combustion. Based on the *in-situ* gaseous volume concentration

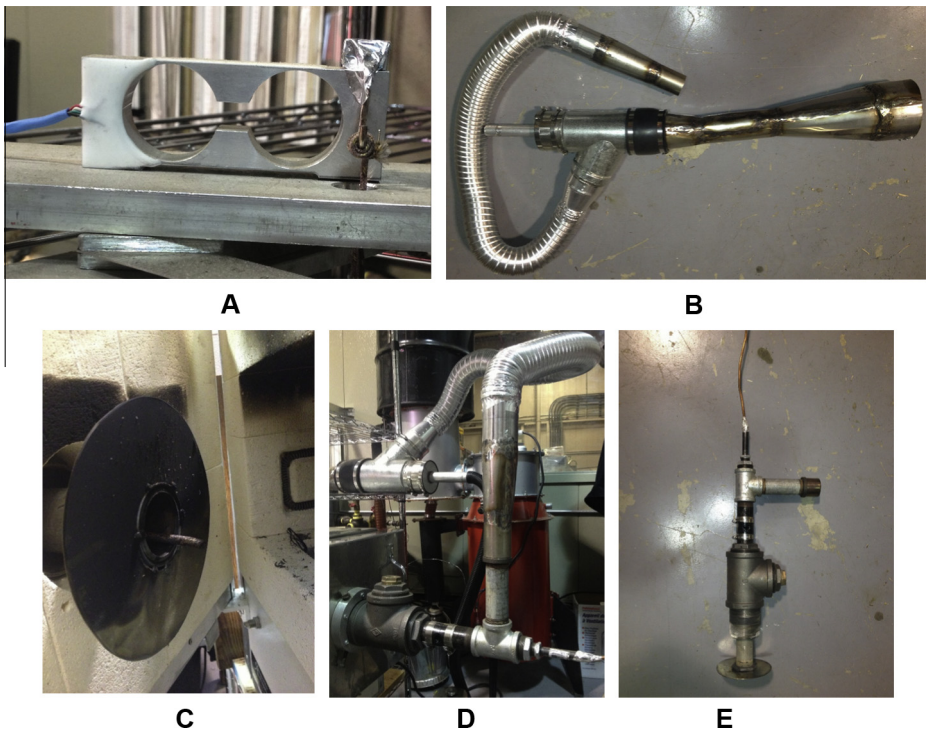

Fig. 2. Photo on the detailed parts of the biomass fuel experimental combustion system. A: Elane 1.2 kg load cell that was used to measure the mass change of fuel sample; B: Bernoulli's principle air ejector; C: Air/exhaust distribution panel inside the combustion chamber; D: Assembled air injection and ejection system; F: Air injector with airflow velocity measuring spot.

Table 1
Experimental design for investigating the effect of different excess air ratio on the combustion of switchgrass and hardwood in the experimental system.

Designation	Fuel	Excess air ratio	External pump voltage (%)	Actual air supply (kg)	Stoichiometric air demand (kg)	Initial fuel load (kg)	Replication
S1.0 (control)	Switchgrass	1.0	0	0.89	0.89	0.20	3
S1.1	Switchgrass	1.1	10	1.03	0.94	0.21	3
S1.2	Switchgrass	1.2	20	1.34	1.12	0.24	3
S1.3	Switchgrass	1.3	30	1.65	1.27	0.28	3
H1.0 (control)	Hardwood	1.0	0	0.89	0.89	0.19	3
H1.1	Hardwood	1.1	10	1.03	0.94	0.19	3
H1.2	Hardwood	1.2	20	1.34	1.12	0.23	3
H1.3	Hardwood	1.3	30	1.65	1.27	0.26	3

$V(t)$ (%) in exhaust measured by gas analyzer, the total CO and CO_2 emissions and O_2 consumption by 90 min combustion were calculated by Eqs. (4) and (5).

$$\text{CO or } CO_2 \text{ total emission} = \frac{5400 \times N \times S \times \int_0^{90} V(t)dt}{100 \times 22.4 \times M_f} \quad (4)$$

$$O_2 \text{ total consumption} = \frac{5400 \times N \times S \times \int_0^{90} 21 - V(t)dt}{100 \times 22.4 \times M_f} \quad (5)$$

where N was the molecular weight of CO, CO_2 and O_2 (g/mol), and S was the volume velocity of exhaust (L/s). M_f corresponded to the weight of fuel load in each batch of tests (g). After the tests, the residues were sampled, and char was separated from ash using a No. 35 sieve (500 μm). Each test was replicated three times.

2.4. Combustion performance evaluation

Energy conversion efficiency (ECE) and combustion completeness rate (CCR) were estimated to compare the combustion performance. By considering the combustion as a "black box" with various calorific inputs and outputs (Fig. S2), ECE (%) referred to the ratio of heat release versus the total calorific inputs (Eq. (6)). Meanwhile, the CCR (%/min) was obtained by Eq. (7) to reveal the speed of fuel mass loss during the 90 min combustion.

$$\text{ECE} = \frac{M_f \times \text{HHV}_f - M_{\text{CO}} \times \text{HHV}_{\text{CO}} - M_{\text{ch}} \times \text{HHV}_{\text{ch}}}{M_f \times \text{HHV}_f} \times 100 \quad (6)$$

$$\text{CCR} = \frac{M_f - M_{\text{ch}} - M_a}{M_f \times 90 \text{ min}} \quad (7)$$

where M_f, M_{CO}, M_{ch} and M_a are the initial fuel mass, total CO emission, char and ash product mass. HHV_f, HHV_{CO} and HHV_{ch} correspond to the HHV of fuel (17.5 MJ/kg switchgrass, 17.7 MJ/kg hardwood), CO (20.5 MJ/kg) and char (29.6 MJ/kg), respectively.

2.5. Ash characterization and fouling/slagging assessment

All of the ash samples from the combustion with 1.0–1.3 EAR underwent fouling and slagging assessment. The mineral composition of ash was analyzed by X-ray fluorescence (XRF) with a PW2400 wavelength dispersive XRF spectrometer. Several empirical indices of the fouling and slagging tendencies were estimated,

including the base-acid ratio (BA), fouling index (FI), slagging index (SI) and slag viscosity ratio (SVR) [36].

2.6. Combustion kinetic analysis

2.6.1. Experimental setup

Kinetic analysis requires experimental data on the thermal decomposition rate, which was collected from the TGA–DSC performed on a NETZSCH TG 449 F3 Jupiter Analyzer. About 18 mg of switchgrass or 36 mg of hardwood (owing to their density difference) was heated to 900 °C (10 °C/min) in air atmosphere (20 mL/min) during the TGA–DSC analysis. Each test was replicated three times.

2.6.2. Kinetic modeling

Kinetic analysis used the Coats–Redfern algorithm with a two-step solid-state reaction model (Fig. S3) [26,29,37]. By assuming the combustion process was governed by the first-order Arrhenius law, the kinetic model was expressed by Eqs. (8)–(10),

$$\alpha = \frac{m_0 - m_t}{m_0 - m_f} \tag{8}$$

$$\frac{d\alpha}{dt} = kf(\alpha) \tag{9}$$

$$k = Aexp\left(\frac{-E_a}{RT}\right) \tag{10}$$

where α is the decomposition rate obtained from the TGA–DSC and m_0, m_t and m_f (mg) represented the initial mass, the mass at time t (min), and the final mass of sample. The function $f(\alpha)$ represents the mechanism functions usually employed for the kinetic study of solid-state reaction, which depends on the chemical reaction/diffusion control or the size and shape of the reacting particles. Additional details on the 14 groups of probable mechanisms of solid-state combustion model, including units associated with each mechanism function, are provided in Table 2. k is the reaction rate, and A (min^{-1}) is the pre-exponential factor. E_a (kJ/mol) corresponds to the activation energy of combustion. R is the gas constant (8.314 J/mol K) and T (K) the absolute temperature. Thus, the kinetic modeling was performed according to Eqs. (11) and (12),

$$g(\alpha) = \int_0^{\alpha} \frac{d\alpha}{f(\alpha)} = \frac{A}{\beta}\int_{T_0}^{T} \exp\left(\frac{-E_a}{RT}\right)dT \tag{11}$$

$$\ln\left[\frac{g(\alpha)}{T^2}\right] = \ln\left[\frac{AR}{\beta E_a}\left(1 - \frac{2RT}{E_a}\right)\right] - \frac{E_a}{RT} \tag{12}$$

where $g(\alpha)$ is the integral function of solid-state reaction mechanism and further described in Table 2. T_0 (K) stands for the initial temperature of TGA–DSC test. β corresponds to the heating rate during TGA–DSC test, at 10 °C/min in this work. For most values of E_a and T generated during combustion, the term $\ln[AR/\beta E_a(1–2RT/E_a)]$ in Eq. (12) is considered to be a constant. A linear regression is attained after plotting $\ln[g(\alpha)/T^2]$ versus $1/T$. Meanwhile, a high linear correlation coefficient ($-R^2$) should be obtained if the $f(\alpha)$ in Table 2 is optimized. Consequently, combustion mechanism and E_a could be acquired by choosing an $-R^2$ that is close to 1.

2.7. Statistical analysis

Comparison of switchgrass and hardwood combustion (effect of excess air) was analyzed statistically using a Fisher's Least Significant Difference (LSD) test (at a 0.05 significant level).

3. Results and discussion

3.1. Physiochemical properties

Initially, switchgrass and hardwood contained 80.6% and 80.0% of volatile content, and 8.21% and 12.7% of fixed carbon by weight, respectively (Table 3(a)). As shown in Table 3(b), the oxygenation of switchgrass (52.2% of oxygen) and hardwood (51.0%) resulted in higher heating values of 17.7 MJ/kg (switchgrass) and 17.5 MJ/kg (hardwood) that are less than the 24.1 MJ/kg reported for coal [38]. Nitrogen and sulfur contents of switchgrass (0.60% of N and 0.06% of S) and hardwood (0.01% of N and 0.02% of S) were much less than a representative coal (1.20% of N and 4.87% of S) [38], suggesting that greater reliance on biomass fuel might reduce NO_x and SO_x emissions compared to the coal. These results were consistent with previous reports in the scientific literature [39].

Molecular formula of switchgrass was $CH_{1.7027}O_{0.9476}N_{0.0125}S_{0.0005}$ (29.1 kg/kmol) and hardwood was $CH_{1.7299}O_{0.8937}N_{0.0002}S_{0.0002}$ (28.0 kg/kmol) (Table 3(c)). Stoichiometric air–fuel ratio (SAFR) was 0.96 for switchgrass and 1.02 for hardwood, which is much lower than fossil fuels such as coal (7.1), natural gas (17.2) and gasoline (14.7) [8]. Their lower SAFR were attributed to the considerably less C but higher H and O contents than fossil fuels. Hardwood had 0.78% ash, which was approximately 5-fold less than switchgrass (4.69%); as well hardwood contained nearly 10-fold less SiO_2 and tended to have lower alkali metal (Na_2O and K_2O) content than switchgrass (Tables 3(a) and 4). The appreciable ash content and presence of alkali metals, SiO_2 and sulfur in these biomass fuels is an indication that fouling and slagging could occur in biomass combustion systems using switchgrass and hardwood [40].

Table 2
14 Groups of probable mechanisms of solid-state combustion model.

Symbol	Mechanism	$f(\alpha)$	$g(\alpha)$
F_1	First-order chemical reaction	$1-\alpha$	$-\ln(1-\alpha)$
F_2	Second-order chemical reaction	$(1-\alpha)^2$	$(1-\alpha)^{-1}-1$
R_1	Limited surface reaction (1 dimension)	1	α
R_2	Limited surface reaction (2 dimension)	$2(1-\alpha)^{1/2}$	$1-(1-\alpha)^{1/2}$
R_3	Limited surface reaction (3 dimension)	$3(1-\alpha)^{2/3}$	$1-(1-\alpha)^{1/3}$
$G–B$	Ginstling–Brounshtein equation	$(3/2)[(1-\alpha)^{-1/3}-1]^{-1}$	$1-(2/3)\alpha-(1-\alpha)^{2/3}$
Zh	Zhuravlev equation	$(3/2)(1-\alpha)^{4/3}[(1-\alpha)^{-1/3}-1]^{-1}$	$[(1-\alpha)^{-1/3}-1]^2$
A_2	Random nucleation and nuclei growth (1 dimension)	$2(1-\alpha)[-\ln(1-\alpha)]^{1/2}$	$[-\ln(1-\alpha)]^{1/2}$
A_3	Random nucleation and nuclei growth (2 dimension)	$3(1-\alpha)[-\ln(1-\alpha)]^{2/3}$	$[-\ln(1-\alpha)]^{1/3}$
$P–T_1$	Prout–Tompkins (0.5 order)	$(1-\alpha)\alpha^{1/2}$	$\ln[(1+\alpha^{1/2})/(1-\alpha^{1/2})]$
$P–T_2$	Prout–Tompkins (1 order)	$(1-\alpha)\alpha$	$\ln[\alpha/(1-\alpha)]$
D_1	Diffusion one-way transport	$1/2\alpha$	α^2
D_2	Diffusion two-way transport	$[-\ln(1-\alpha)]^{-1}$	$\alpha+(1-\alpha)\ln(1-\alpha)$
D_3	Diffusion three-way transport	$(3/2)(1-\alpha)^{2/3}[1-(1-\alpha)^{1/3}]^{-1}$	$[1-(1-\alpha)^{1/3}]^2$

Table 3
Properties of switchgrass and hardwood used in the experimental combustion system. (a) Proximate analysis; (b) ultimate analysis and calorific value (higher heating value, MJ/kg); (c) molecular formula and mass (kg/kmol), and stoichiometric air–fuel ratio (SAFR) at stoichiometric combustion condition.

Fuel	Basis	Moisture wt.%	Volatile matter wt.%	Ash wt.%	Fixed carbon wt.%
(a)					
Switchgrass	Air	6.55	80.6	4.69	8.21
	Dry	—	86.2	5.02	8.78
Hardwood	Air	6.51	80.0	0.78	12.7
	Dry	—	85.6	0.83	13.6

Fuel	C wt.%	H wt.%	N wt.%	S wt.%	O wt.%	Higher heating value (HHV) MJ/kg
(b)						
Switchgrass	41.3	5.86	0.60	0.06	52.2	17.5
Hardwood	42.8	6.17	0.01	0.02	51.0	17.7

Fuel	Molecular formula	Molecule mass kg/kmol	Stoichiometric air–fuel ratio (SAFR)
(c)			
Switchgrass	$CH_{1.7027}O_{0.9476}N_{0.0125}S_{0.0005}$	29.1	0.96
Hardwood	$CH_{1.7299}O_{0.8937}N_{0.0002}S_{0.0002}$	28.0	1.02

3.2. Effect of excess air on fuel combustion

The mean yield of ash and char were affected by different EAR (Fig. 3 and Table S1). Hardwood combustion consistently generated less residues (1.01–1.27% of ash and 1.61–2.50% of char, by weight) than switchgrass (3.19–4.94% ash and 3.82–5.73% of char). Higher char yield of switchgrass can be explained by the ash coagulation, whereby ash agglomerates with unburned carbon [41,42]. Because the char was separated by screening, some agglomerated ash was categorized as the char, which could be increasing the apparent char yield from switchgrass combustion. Compared to the control group, more excess air (10–30%) boosted the combustion completeness and reduced the amount of unburned residues. As for the switchgrass, there was no significant difference in the ash yield from 1.0 EAR (4.93%) and 1.1 EAR (4.94%) tests ($P = 0.90$). Ash yield declined to 4.20% and 3.18% with more air supply (1.2 and 1.3 EAR) and the lowest char production (3.82%) occurred at 1.2 EAR compared to the other excess air levels, which was interpreted to mean that more complete switchgrass combustion was achieved at 1.2 EAR condition. Regarding the hardwood, there was no statistically significant difference in the ash yield from among the 1.0, 1.2 and 1.3 EAR treatments (Fig. 3). Increasing the EAR from 1.0 to 1.1 reduced the char yield significantly ($P = 5.84E{-}4$), from 2.50% to 1.87%. Yet, continuing to increase the EAR to 1.3 resulted in no further reduction in char yield. This observation indicates that 10% of excess air was sufficient for a complete hardwood combustion.

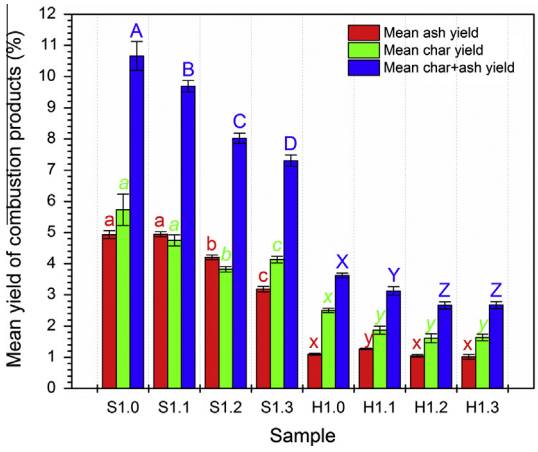

Fig. 3. Mean yield (wt.%) of the ash and char combustion products from combustion tests, presented separately and as the sum of ash + char. Samples are labeled as S = switchgrass or H = hardwood that were combusted with an excess air ratio of 1.0 (stoichiometric conditions), 1.1, 1.2 or 1.3. Columns with different letters were significantly different at $P < 0.05$ level, assessed by a Fisher's LSD test.

Mass loss profiles follow a predictable pattern, where the first stages of combustion result in early moisture removal (minor mass loss), followed by fast volatile separation (dramatic mass loss) and slow char oxidation (gentle mass loss) [8]. Increasing the EAR altered the mass loss profile of switchgrass, compared to stoichiometric conditions (1.0 EAR) during the fast volatile separation step (up to 65 min in the combustion), such that greater mass loss due to volatile combustion occurred when the EAR was set at 1.2 and 1.3 (Fig. 4(a)). By contrast, the major variance in hardwood mass loss profiles at various EAR occurred from 0 to 20 min (Fig. 4(b)). This indicated that excess air injected in the combustion system accelerated the early steps of fast volatile separation of hardwood in the first 20 min following ignition. Thereafter, mass loss was slower with EAR above 1 than the stoichiometric condition, although all mass loss curves converged from 50 to 90 min indicating that the late char oxidation phase was unaffected by EAR during hardwood combustion.

Combustion temperature measured in the fuel holder was always lower at the top (e.g., from 523 to 662 °C with switchgrass; Table 5) than the bottom (882–1129 °C with switchgrass) because the top of the fuel holder encountered an intense convective heat transfer effect. The greatest combustion temperatures for switchgrass were achieved with 1.1 EAR. This disparity was also be observed in the hardwood combustion test, where temperatures at the top of the fuel holder were generally lower than those at the bottom (Table 5). The greatest combustion temperatures were reached at 1.3 EAR (821 °C at the bottom of the fuel holder) and 1.0 EAR (735 °C at the top of the fuel holder).

Since oxygen supply for combustion was determined by the excess air amount, the total CO and CO_2 emissions as well as O_2 consumption were related to the EAR (Fig. 5). Consequently, CO_2 emission and O_2 consumption were greater with a higher EAR during the combustion of switchgrass. Simultaneously, the 1.3 EAR

Table 4
Major mineral oxides and trace metal elements (wt.%) in switchgrass and hardwood used in the experimental combustion system.

Elements	Unit	Switchgrass	Hardwood
Major mineral oxides			
SiO_2	wt.%	2.23	0.23
Al_2O_3	wt.%	0.25	0.03
Fe_2O_3	wt.%	0.20	0.04
MnO	wt.%	0.01	0.02
MgO	wt.%	0.08	0.04
CaO	wt.%	0.56	0.24
Na_2O	wt.%	0.04	0.01
K_2O	wt.%	0.14	0.11
TiO_2	wt.%	0.01	0.00
P_2O_5	wt.%	0.09	0.02
Loss on ignition (LOI)	wt.%	96.4	99.4
Trace metal elements			
Ba	ppm	39	23
Sr	ppm	21	10
Y	ppm	<1	<1
Sc	ppm	<1	<1
Zr	ppm	3	3
Be	ppm	<1	<1
V	ppm	<5	<5

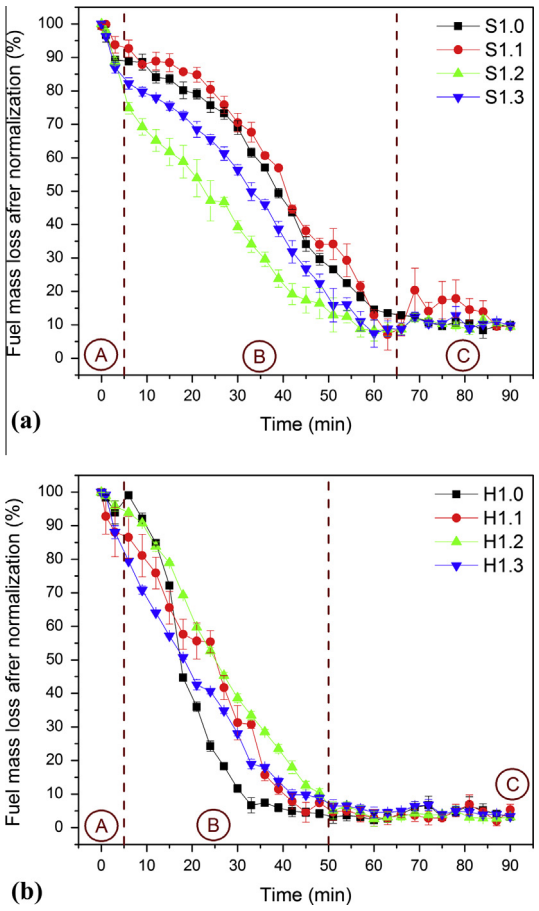

Fig. 4. Mass loss profile during a 90 min combustion of switchgrass (a) or hardwood (b) with excess air ratios of 1.0, 1.1, 1.2 and 1.3, which received 0%, 10%, 20% and 30% excess air intake, respectively. Samples are labeled as S = switchgrass or H = hardwood that were combusted with an excess air ratio of 1.0 (stoichiometric conditions), 1.1, 1.2 or 1.3. The mass loss is divided into three phases, including A: early moisture removal, B: fast volatile separation, and C: slow char oxidization.

level gave a significantly higher CO emission (18.0%) than 1.0 EAR (16.9%, $P = 0.02$), 1.1 EAR (16.5%, $P = 0.01$) and 1.2 EAR tests (16.7%, $P = 0.01$). A probable explanation was that more CO was formed from char oxidization at 30% of excess air, but there was insufficient oxygen in the air supply to oxidize the extra CO. In contrast, the CO emission from hardwood combustion diminished significantly ($P = 0.01$) from 8.72% (kg gas/kg fuel) to 5.38% as the EAR increased from 1.0 to 1.3. Accordingly, more excess air augmented the CO_2 emission from 9.88% (1.0 EAR) to 36.8% (1.3 EAR), and the total O_2 consumption also increased from 16.9% at 1.0 EAR to 31.8%

Table 5
Highest temperature (mean ± standard deviation) measured at the bottom and top of fuel holder in the 90 min combustion of switchgrass (a) or hardwood (b) with different excess air ratio (1.0, 1.1, 1.2 and 1.3).

Designation	Highest combustion temperature (°C)			
	Bottom		Top	
	Average	Standard deviation	Average	Standard deviation
S1.0 (control)	905	20.5	523	3.3
S1.1	1129	35.9	662	23.7
S1.2	938	18.8	576	11.4
S1.3	882	24.5	528	13.1
H1.0 (control)	386	9.8	735	22.2
H1.1	762	22.5	673	15.2
H1.2	801	19.3	709	19.6
H1.3	821	17.2	721	13.0

with 1.3 EAR. These results indicate that 1.3 EAR assured complete hardwood combustion in the experimental combustion system.

However, the incompleteness of combustion was evidently observed from the results above even when 10–30% excess air was supplied. For instance, theoretically there should not be any char products (Fig. 3), or the O_2 consumption should be unchanged if the combustion is actually completed with 10–30% excess air (Fig. 5). These contradictions were attributed to the physical limitations of our combustion system, in contrast with an ideal manner that only used a single fine particle of fuel at a perfect air supply condition. Despite the fine particle size of fuel (4 mm), there were still many factors that resulted in heat and mass transfer delays, which made the fuel unable to react with air rapidly and completely in 90 min. Yet, compared to any ideal tests that mostly entirely eliminated these deficiencies, the findings by this research was particularly valuable for real boiler, since heat and mass transfer delays were an inevitable phenomenon in any large-scale operations. Therefore, aside from the research above, we should further assess the influence on energy conversion and combustion completeness to find the optimal EAR for this combustion system.

3.3. Energy conversion efficiency (ECE) and combustion completeness rate (CCR) as affected by excess air

Numerically, the highest ECE for switchgrass was 75.1% at 1.2 EAR, which was not statistically different from the ECE at other

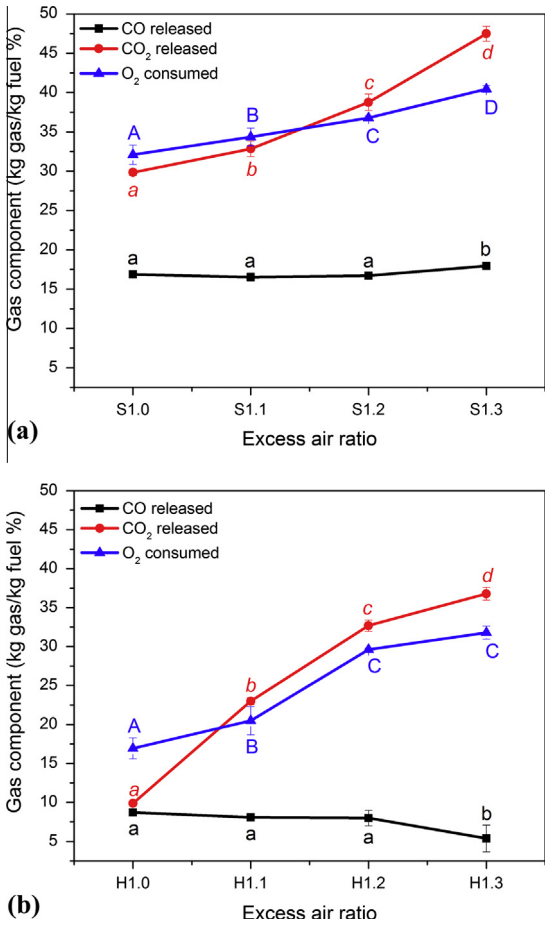

Fig. 5. Total CO and CO_2 released, and O_2 consumed (kg gas/kg fuel, %) during the 90 min combustion of switchgrass (a) or hardwood (b) with excess air ratios of 1.0, 1.1, 1.2 and 1.3 respectively. Samples are labeled as S = switchgrass or H = hardwood that were combusted with an excess air ratio of 1.0 (stoichiometric conditions), 1.1, 1.2 or 1.3. Points on each curve with different letters were significantly different at the $P < 0.05$ level, assessed by a Fisher's LSD test.

EAR levels (Fig. 6). Switchgrass consistently exhibited lower energy efficiency than hardwood due to the higher char yield of switchgrass than hardwood in the experimental combustion system. With a calorific output of 29.6 MJ/kg (Fig. S2), char formation reduced the heat release, thus reducing the energy conversion. Since the CCR of switchgrass reached a maximum between 1.1 EAR (0.421%/min) and 1.2 EAR (0.410%/min), we suggest that 20% of excess air would be optimal to achieve the highest ECE and CCR for switchgrass, while simultaneously lowering the mass of char and ash produced, relative to the 1.0 and 1.1 EAR levels, in the experimental combustion system.

Compared to the control group of hardwood, which had an ECE of 85.7% at 1.0 EAR, there was no significant difference in the ECE at 1.1 EAR (87.5%, $P = 0.14$) or 1.2 EAR test (88.0%, $P = 0.07$) (Fig. 6). Yet, the 1.3 EAR remarkably enhanced the ECE to 91.0% ($P = 0.03$, compared to the 1.2 EAR test). This higher energy output produced the highest flame temperature (821 °C at the bottom of the fuel holder, Table 5), presumably because fast volatile separation and slow char oxidization processes were both exothermic. Moreover, excess air accelerated the CCR from 0.471%/min (1.0 EAR) to a maximum of 0.537%/min (1.2 EAR) and 0.535%/min (1.3 EAR), the latter two measurements being similar ($P = 0.75$). The slowest CCR of 0.404%/min measured at 1.1 EAR implies that 10% of excess air was insufficient for the complete combustion of hardwood while air intake causes heat transfer and a "cooling effect" that reduces the flame temperature at the top of the fuel holder, relative to the control group (Table 5). This is consistent with other reports that hardwood combustion at 1.1 EAR was controlled by limited oxygen availability and adversely affected by heat transfer, including conductive, convective and radiative effect [43,44]. Consequently, 30% of excess air was recommended to obtain the greatest energy efficiency during hardwood combustion in our experimental system.

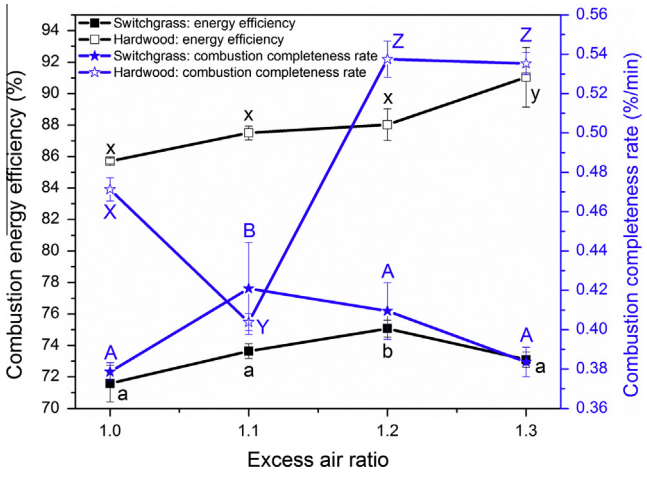

Fig. 6. Energy conversion efficiency (%) and combustion completeness rate (%/min) during the 90 min combustion of switchgrass (a) or hardwood (b) with different excess air ratio (1.0, 1.1, 1.2 and 1.3). Points on each curve with different letters were significantly different at the $P < 0.05$ level, assessed by a Fisher's LSD test.

3.4. Fouling and slagging assessment

The fouling and slagging potential of biomass fuel is a function of the chemical composition of its ash, particularly the Na_2O, K_2O and SiO_2 contents. All of the ashes from the 1.0 to 1.3 EAR combustion tests were chemically compared for this evaluation. Hardwood ash contained substantially less SiO_2 (11.2–13.1% by weight) but more alkali metals (5.2–8.0% $Na_2O + K_2O$) than switchgrass ash (62.7–67.6% SiO_2, 1.2–1.4% $Na_2O + K_2O$) (Table 6), meaning that switchgrass ash was more acidic, which lowers the risk of fouling and slagging in combustion systems [45]. Consequently, the basic-acid ratio (BA) of hardwood (1.9–3.3) was more than 10-fold higher than switchgrass (0.2–0.3). Hardwood ash had a medium fouling index (FI) of 9.7–26.5 and switchgrass ash had a minor FI of 0.2–0.7. The slagging index (SI) of hardwood (3.8–6.6) was likewise considerably higher than switchgrass (1.1–2.0), although the slag viscosity ratio (SVR) of switchgrass was much higher than hardwood due to the high SiO_2 content in its ash. In summary, switchgrass had lower potential of fouling and slagging in a biomass combustion system than hardwood.

Different combustion conditions may not obviously influence the chemical composition and fouling and slagging assessment of ash. For instance, although different EAR altered the char and ash yield proportions, the chemical composition of ash would be

Table 6
Mineral oxide component (wt.%) and fouling and slagging indices estimated by empirical equations of the ash from the combustion of switchgrass and hardwood at an excess air ratio of 1.0, 1.1, 1.2 and 1.3.

Mineral oxides (wt.%)		S1.0	S1.1	S1.2	S1.3	H1.0	H1.1	H1.2	H1.3
SiO_2		62.7	63.4	65.4	67.6	12.8	12.5	11.2	13.1
Al_2O_3		0.7	0.8	0.7	0.7	2.4	1.5	2.4	3.2
Fe_2O_3		0.3	0.7	0.7	0.3	1.5	1.2	2.0	2.4
MgO		2.2	2.1	2.7	2.0	3.6	2.8	5.0	5.2
CaO		8.3	16.6	8.1	11.8	22.2	17.3	30.7	34.4
Na_2O		0.1	0.1	0.1	0.1	0.8	0.7	0.8	1.3
K_2O		1.1	1.9	1.5	1.3	6.2	4.5	7.2	5.3
Indices	Empirical equation								
Base-acid ratio (B/A)	$(Fe_2O_3 + CaO + MgO + K_2O + Na_2O)/(SiO_2 + TiO_2 + Al_2O_3)$	Low (0.2)	Low (0.3)	Low (0.2)	Low (0.2)	High (2.2)	High (1.9)	High (3.3)	High (3.0)
Fouling index (FI)	$BA \times (K_2O + Na_2O)$	Low (0.2)	Medium (0.7)	Low (0.3)	Low (0.3)	Medium (15.5)	Medium (9.7)	Medium (26.5)	Medium (19.7)
Slagging index (SI)	$BA \times S^{d}$[a]	Medium (1.1)	Medium (2.0)	Medium (1.2)	Medium (1.4)	High (4.5)	High (3.8)	High (6.6)	High (5.9)
Slag viscosity ratio (SVR)	$100 \times SiO_2/(SiO_2 + Fe_2O_3 + CaO + MgO)$	High (84.8)	High (76.5)	High (85.2)	High (82.4)	Low (31.2)	Low (36.7)	Low (22.8)	Low (23.4)

Base-acid ratio (B/A): <0.5 low, 0.5–1.0 medium, >1.0 high.
Fouling index (FI): <0.6 low, 0.5–40 medium, >40 high.
Slagging index (SI): <0.6 low, 0.6–2.0 medium, >2.0 high.
Slag viscosity ratio (SVR): <65 low, 65–72 medium, >72 high.
[a] S^{d} corresponded to the sulfur content in dried initial fuel, and others referred to the mineral oxide content in ash.

constant as long as the ash was completely separated from char particles. To avoid interference from char, the ash composition is best measured in a case when complete combustion occurred (all solid-phase carbon was transformed to a gaseous phase). This statement is reinforced by our previous study [23], where the switchgrass ash was produced from a much larger-scale furnace combustion (84 cm × 38 cm × 51 cm). Its chemical composition (e.g. 67.2% SiO_2 and 1.4% $Na_2O + K_2O$) was comparable to the results in this study. Regarding the ash produced from the same fuel under different EAR conditions, the variation of their chemical composition and accordingly the fouling and slagging tendencies was attributed to the experimental error when manually separating the ash from unburned char. More importantly, as the empirical equations of fouling and slagging tendencies in Table 6 exclusively relied on the chemical composition of initial fuel and ash, these assessment results should be independent of combustion conditions, such as combustor type, mode and scale. Therefore, these assessment results achieved by this study were also applicable to other commercialized operations (e.g. boiler or fixed bed).

3.5. Combustion kinetics

3.5.1. TGA–DSC results

Switchgrass and hardwood combustion exhibited a similar mass loss (Fig. 7), which consists of three steps: moisture removal (28–261 °C switchgrass, 26–262 °C hardwood), fast volatile separation (261–364 °C switchgrass, 262–366 °C hardwood) and slow char oxidization (364–861 °C switchgrass, 366–862 °C hardwood) (Table 7). A similar TGA profile for switchgrass was also obtained by Fahmi et al. [46] and Szemmelveisz et al. [47]. Maximal thermal decomposition rate (D_{max}) of hardwood (−2.40%/°C) was faster than switchgrass (−1.68%/°C). Fast volatile separation was the period of highest mass loss (54.0% switchgrass, 60.1% hardwood), but did not release much energy (1.11 kJ/g switchgrass, 0.710 kJ/g hardwood). Energy release was greatest during the slow char oxidization phase (7.09 kJ/g for switchgrass, 4.09 kJ/g for hardwood). Thus, complete combustion is necessary to achieve the greatest energy conversion from biomass fuel, as illustrated in Fig. 6.

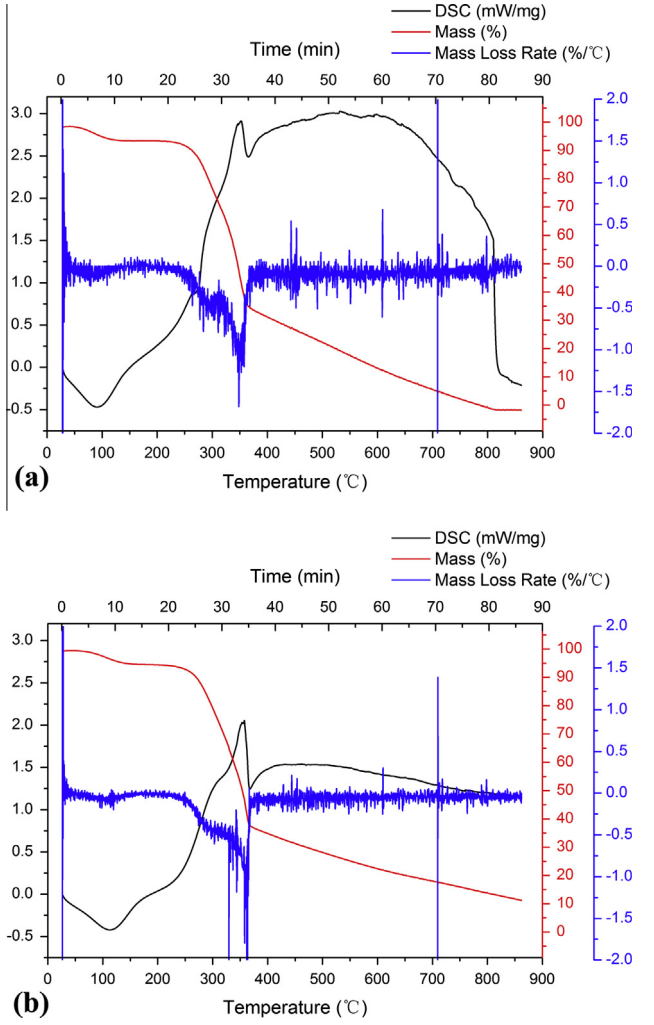

Fig. 7. Non-isothermal thermogravimetric analysis–differential scanning calorimetry (TGA–DSC) profile of switchgrass (a) or hardwood (b).

3.5.2. Kinetic analysis results

Kinetic analysis of the combustion process was performed with a two-step reaction model (Fig. S3) that described the fast volatile separation and slow char oxidization steps according to the experimental temperatures achieved from the TGA–DSC analysis of switchgrass and hardwood. The reliability of kinetic results was confirmed by the high $-R^2$ values, from 0.9785 to 0.9997 (Tables 8 and S2). The mechanisms describing the fast volatile separation phase of switchgrass and hardwood were diffusion two-way transport (D_2) and the Ginstling–Brounshtein equation (GB), respectively. Hardwood had a smaller E_a (94.1 kJ/mol) than switchgrass (103 kJ/mol), which means that the volatile separation of compounds contained in hardwood occurred at a lower activation energy than those contained in switchgrass. This different was probably due to the lower oxygen content in hardwood (51.0%) than switchgrass (52.2%). Both switchgrass and hardwood had lower E_a values in the slow char oxidization phase, which was described by the mechanisms of diffusion two-way transport (D_2) (2.29 kJ/mol) and diffusion three-way transport (D_3) (3.77 kJ/mol). This indicated that char oxidization was expected to progress easily after the volatile separation phase, and it should not be limited by the rates at which chemical bonds were broken to release energy in an oxygen-rich environment [48]. This is another reason why increasing oxygen availability during the combustion process should be advantageous to achieve complete energy conversion from biomass

Table 7
Critical parameters of non-isothermal thermogravimetric analysis–differential scanning calorimetry (TGA–DSC) of switchgrass or hardwood.

Parameter		Unit	Switchgrass	Hardwood
Maximal decomposition rate (D_{max})		%/°C	−1.68	−2.40
Maximal decomposition rate temperature (T_{max})		°C	348	362
Total enthalpy release		kJ/g	8.15	4.63
Temperature zone		°C	26–262	28–261
Conversion rate	Step 1: moisture removal	%	9.53	9.46
Heat release		kJ/g	−0.17	−0.05
Temperature zone		°C	262–366	261–364
Conversion rate	Step 2: fast volatile separation	%	60.1	54.0
Heat release		kJ/g	0.71	1.11
Temperature zone		°C	366–862	364–861
Conversion rate	Step 3: slow char oxidization	%	30.4	36.5
Heat release		kJ/g	4.09	7.09

Table 8
Kinetic parameters, E_a (activation energy of combustion) and A (pre-exponential factor), and mechanisms describing switchgrass and hardwood combustion based on thermogravimetric kinetic analysis with the Coats–Redfern algorithm in a two-step solid-state reaction model. Goodness of fit ($-R^2$) is provided for models of the fast volatile separation and late char oxidation phases for each biomass fuel.

Fuel	Switchgrass						Hardwood					
Stage	Fast volatile separation			Slow char oxidization			Fast volatile separation			Slow char oxidization		
Kinetic parameters	E_a	A	$-R^2$	E_a	A	$-R^2$	E_a	A	$-R^2$	E_a	A	$-R^2$
	kJ/mol	/min	1	kJ/mol	/min	1	kJ/mol	/min	1	kJ/mol	/min	1
	103	2.67E+07	0.9988	2.29	2.83E−03	0.9785	94.1	1.14E+06	0.9993	3.77	2.44E−03	0.9939
Mechanism/equation	Diffusion two-way transport			Diffusion two-way transport			Ginstling–Brounshtein equation			Diffusion three-way transport		

4. Conclusions

Specific to our laboratory combustion system, 20% excess air for switchgrass or 30% excess air for hardwood would optimize the combustion, resulting in the highest energy conversion and combustion completeness rate. Switchgrass was less likely to create fouling and slagging problems than hardwood, owing to its more acidic chemical composition. Kinetic analysis pointed to the need to increase the oxygen availability to achieve better energy conversion efficiency from biomass.

Key results of this study that are informative for commercial operations such as boiler combustion are as follows:

(1) The curves of the fuel mass loss, temperatures and gaseous emissions versus time can be used for providing computational fluid dynamic simulation of boilers with kinetic data; (2) Fouling and slagging assessment results were independent of combustion conditions and combustor types, thus are applicable to the boiler operation; (3) The TGA–DSC results also pinpointed the best temperature zone for boiler combustions.

However, there are still some physical limitations in our combustion system that we still cannot utterly avoid, particularly the heat and mass transfer delays. These delays retarded the combustion even if an excess air was supplied. Yet, this phenomenon is fairly common when the combustion is conducted in a commercial-scale boiler, which should not be entirely eliminated in any laboratory-scale studies. Further studies should be expanded to consider (1) a single particle fuel test at an ideal condition without any heat and mass transfer delays, and (2) a boiler test for experimental verification of the assertions made in this study.

Acknowledgments

This research was funded by Natural Science and Engineering Research Council (NSERC) of Canada, and the McGill Collaborative Research Development Fund. We also appreciate the industrial support of Lafarge Cement North America.

Appendix A. Supplementary material

Supplementary data associated with this article can be found, in the online version, at http://dx.doi.org/10.1016/j.enconman.2015.03.070.

References

[1] Demirbas MF, Balat M, Balat H. Potential contribution of biomass to the sustainable energy development. Energy Convers Manage 2009;50:1746–60.
[2] Cherubini F. The biorefinery concept: using biomass instead of oil for producing energy and chemicals. Energy Convers Manage 2010;51:1412–21.
[3] Zhang L, Xu CC, Champagne P. Overview of recent advances in thermochemical conversion of biomass. Energy Convers Manage 2010;51:969–82.
[4] Pantaleo AM, Giarola S, Bauen A, Shah N. Integration of biomass into urban energy systems for heat and power. Part I: An MILP based spatial optimization methodology. Energy Convers Manage 2014;83:347–61.
[5] Demirbaş A. Biomass resource facilities and biomass conversion processing for fuels and chemicals. Energy Convers Manage 2001;42:1357–78.
[6] Demirbas A. Combustion characteristics of different biomass fuels. Prog Energy Combust Sci 2004;30:219–30.
[7] Varol M, Atimtay AT, Olgun H, Atakül H. Emission characteristics of co-combustion of a low calorie and high sulfur-lignite coal and woodchips in a circulating fluidized bed combustor: Part 1. Effect of excess air ratio. Fuel 2014;117:792–800.
[8] Nussbaumer T. Combustion and co-combustion of biomass: fundamentals, technologies, and primary measures for emission reduction. Energy Fuels 2003;17:1510–21.
[9] Steer J, Marsh R, Griffiths A, Malmgren A, Riley G. Biomass co-firing trials on a down-fired utility boiler. Energy Convers Manage 2013;66:285–94.
[10] Pronobis M, Wojnar W. The impact of biomass co-combustion on the erosion of boiler convection surfaces. Energy Convers Manage 2013;74:462–70.
[11] Teixeira P, Lopes H, Gulyurtlu I, Lapa N, Abelha P. Slagging and fouling during coal and biomass cofiring: chemical equilibrium model applied to FBC. Energy Fuels 2013;28:697–713.
[12] Wang C, Xu C, Cao Z, Di H. Investigation on minerals migration during co-firing of different straw/coal blending ratios. Energy Convers Manage 2013;74:279–85.
[13] Teixeira P, Lopes H, Gulyurtlu I, Lapa N, Abelha P. Evaluation of slagging and fouling tendency during biomass co-firing with coal in a fluidized bed. Biomass Bioenergy 2012;39:192–203.
[14] Tortosa Masiá A, Buhre B, Gupta R, Wall T. Characterising ash of biomass and waste. Fuel Process Technol 2007;88:1071–81.
[15] Degereji M, Gubba S, Ingham D, Ma L, Pourkashanian M, Williams A, et al. Predicting the slagging potential of co-fired coal with sewage sludge and wood biomass. Fuel 2013;108:550–6.
[16] Wang Y, Winans KS, Shao Y, Matovic MD, Whalen JK. Life cycle assessment of biomass integrated gasification combined cycle in cement industry. In: The seventh international conference on environmental science and technology, Houston, Texas, USA; 2014.
[17] Kumar A, Sokhansanj S. Switchgrass (*panicum vigratum, L.*) delivery to a biorefinery using integrated biomass supply analysis and logistics (IBSAL) model. Bioresource Technol 2007;98:1033–44.
[18] Vamvuka D, Topouzi V, Sfakiotakis S. Evaluation of production yield and thermal processing of switchgrass as a bio-energy crop for the Mediterranean region. Fuel Process Technol 2010;91:988–96.
[19] Forbes E, Easson D, Lyons G, McRoberts W. Physico-chemical characteristics of eight different biomass fuels and comparison of combustion and emission results in a small scale multi-fuel boiler. Energy Convers Manage 2014;87:1162–9.
[20] McKendry P. Energy production from biomass (part 1): overview of biomass. Bioresource Technol. 2002;83:37–46.
[21] Ogden C, Ileleji K, Johnson K, Wang Q. In-field direct combustion fuel property changes of switchgrass harvested from summer to fall. Fuel Process Technol 2010;91:266–71.
[22] Amaral SS, de Carvalho Junior JA, Costa MAM, Neto TGS, Dellani R, Leite LHS. Comparative study for hardwood and softwood forest biomass: chemical characterization, combustion phases and gas and particulate matter emissions. Bioresource Technol 2014;164:55–63.
[23] Wang Y, Shao Y, Matovic MD, Whalen JK. Recycling of switchgrass combustion ash in cement: characteristics and pozzolanic activity with chemical accelerators. Constr Build Mater 2014;73:472–8.
[24] Wang Y, Shao Y, Matovic MD, Whalen JK. Optimization of switchgrass combustion for simultaneous production of energy and pozzolan. J Mater Civil Eng 2015. http://dx.doi.org/10.1061/(ASCE)MT.1943-5533.0001312.
[25] Kok MV. Simultaneous thermogravimetry–calorimetry study on the combustion of coal samples: effect of heating rate. Energy Convers Manage 2012;53:40–4.
[26] White JE, Catallo WJ, Legendre BL. Biomass pyrolysis kinetics: a comparative critical review with relevant agricultural residue case studies. J Anal Appl Pyrolysis 2011;91:1–33.
[27] Várhegyi G. Aims and methods in non-isothermal reaction kinetics. J Anal Appl Pyrolysis 2007;79:278–88.
[28] Vyazovkin S, Wight C. Kinetics in solids. Annu Rev Phys Chem 1997;48:125–49.

[29] Gil M, Casal D, Pevida C, Pis J, Rubiera F. Thermal behaviour and kinetics of coal/biomass blends during co-combustion. Bioresource Technol 2010;101:5601–8.
[30] Fang X, Jia L, Yin L. A weighted average global process model based on two-stage kinetic scheme for biomass combustion. Biomass Bioenergy 2013;48:43–50.
[31] Kuprianov VI, Arromdee P. Combustion of peanut and tamarind shells in a conical fluidized-bed combustor: a comparative study. Bioresource Technol 2013;140:199–210.
[32] Xiao H, Ma X, Liu K. Co-combustion kinetics of sewage sludge with coal and coal gangue under different atmospheres. Energy Convers Manage 2010;51:1976–80.
[33] Aboulkas A, El Bouadili A. Thermal degradation behaviors of polyethylene and polypropylene. Part I: Pyrolysis kinetics and mechanisms. Energy Convers Manage 2010;51:1363–9.
[34] Yang YB, Ryu C, Khor A, Yates NE, Sharifi VN, Swithenbank J. Effect of fuel properties on biomass combustion. Part II. Modelling approach-identification of the controlling factors. Fuel 2005;84:2116–30.
[35] Rahman F, Umesh D, Subbarao D, Ramasamy M. Enhancement of entrainment rates in liquid-gas ejectors. Chem Eng Process 2010;49:1128–35.
[36] Barroso J, Ballester J, Pina A. Study of coal ash deposition in an entrained flow reactor: assessment of traditional and alternative slagging indices. Fuel Process Technol 2007;88:865–76.
[37] Sahin Ö, Özdemir M, Aslanoglu M, Beker ÜG. Calcination kinetics of ammonium pentaborate using the Coats–Redfern and genetic algorithm method by thermal analysis. Ind Eng Chem Res 2001;40:1465–70.
[38] Weiland NT, Means NC, Morreale BD. Product distributions from isothermal co-pyrolysis of coal and biomass. Fuel 2012;94:563–70.
[39] Hu Z, Sykes R, Davis MF, Brummer EC, Ragauskas AJ. Chemical profiles of switchgrass. Bioresource Technol 2010;101:3253–7.
[40] Jenkins B, Baxter L, Miles Jr T, Miles T. Combustion properties of biomass. Fuel Process Technol 1998;54:17–46.
[41] Lind T, Vaimari T, Kauppinen E, Nilsson K, Sfiris G, Maenhaut W. Ash formation mechanisms during combustion of wood in circulating fluidized beds. Proc Combust Inst 2000;28:2287–95.
[42] McLennan A, Bryant G, Stanmore B, Wall T. Ash formation mechanisms during pf combustion in reducing conditions. Energy Fuels 2000;14:150–9.
[43] Ryu C, Yang YB, Khor A, Yates NE, Sharifi VN, Swithenbank J. Effect of fuel properties on biomass combustion: Part I. Experiments-fuel type, equivalence ratio and particle size. Fuel 2006;85:1039–46.
[44] Smart JP, Patel R, Riley GS. Oxy-fuel combustion of coal and biomass, the effect on radiative and convective heat transfer and burnout. Combust Flame 2010;157:2230–40.
[45] Vamvuka D, Pitharoulis M, Alevizos G, Repouskou E, Pentari D. Ash effects during combustion of lignite/biomass blends in fluidized bed. Renewable Energy 2009;34:2662–71.
[46] Fahmi R, Bridgwater A, Darvell L, Jones J, Yates N, Thain S, et al. The effect of alkali metals on combustion and pyrolysis of Lolium and Festuca grasses, switchgrass and willow. Fuel 2007;86:1560–9.
[47] Szemmelveisz K, Szűcs I, Palotas A, Winkler L, Eddings E. Examination of the combustion conditions of herbaceous biomass. Fuel Process Technol 2009;90:839–47.
[48] Sait HH, Hussain A, Salema AA, Ani FN. Pyrolysis and combustion kinetics of date palm biomass using thermogravimetric analysis. Bioresource Technol 2012;118:382–9.